npg

Redox survival signalling in retina-derived 661W cells

AM Mackey[1], N Sanvicens[1], G Groeger[1], F Doonan[1], D Wallace[1] and TG Cotter*[,1]

Reactive oxygen species have been implicated in processes involving cellular damage and subsequent cell death, especially in organs such as the eye that are constantly exposed to excitatory signals. However, recent studies have shown that oxidant species can also act as intracellular signalling molecules promoting cell survival, but little is known about this mechanism in the retina. The present study demonstrates for the first time that hydrogen peroxide (H_2O_2) is generated rapidly and acts as a pro-survival signal in response to a variety of apoptotic stimuli in retina-derived 661W cells and in the retinal ganglion cell line RGC-5. Focussing on 661Ws and serum deprivation, we systematically investigated pro-survival and pro-death pathways and discovered that the rapid and transient burst of H_2O_2 activates the AKT survival pathway. Activation of the apoptotic machinery takes place following the decline of H_2O_2 to basal levels. To substantiate this proposed pro-survival role of H_2O_2, we inhibited the oxidant burst, which exacerbated cell death. Conversely, maintenance of the oxidant signal using exogenous H_2O_2 enhanced cell survival. Overall, the results presented in this study provide evidence for a novel role of H_2O_2 in mediating survival of retinal cells in response to apoptotic stimuli.

Reactive oxygen species (ROS) comprise a variety of molecular entities that are found in normal cells as a result of oxygen consumption. Among ROS, hydrogen peroxide (H_2O_2) is a rather stable molecule that is continuously generated in the cell during respiration due to the activity of enzymes such as superoxide dismutase or the NADPH oxidase system. When an imbalance between cellular production and elimination of free radical species occurs, cells undergo oxidative stress.

The traditional view of oxidative stress is that it causes cellular damage and subsequent cell death. These observations have led to the association of ROS with pathological conditions and disease, especially in organs such as the brain and eye, which are constantly exposed to excitatory signals and have high oxygen consumption rates. Indeed, high oxidant levels have been detected in numerous neurological and retinal disorders.[1,2] For example, in the nervous system, dopamine-derived H_2O_2 is one of the agents responsible for the damage observed in the brain of Parkinson's disease patients,[3] and in Alzheimer's disease, H_2O_2 mediates amyloid β protein toxicity.[4] In the eye, it is well established that H_2O_2 is the major oxidant contributing to cataract formation[5] and is capable of altering several structures of the eye in disorders, such as glaucoma[1] and age-related macular degeneration.[6]

Contrary to the traditional concept of oxygen species as a cell death-triggering force, recent work has shown that ROS can also act as intracellular signalling molecules.[7,8] For example, oxidant generation is essential to maintain homoeostasis in the cell[9] and is involved in regulating gene expression and modulating enzyme activities.[10] Therefore, H_2O_2 is not simply a by-product of enzymatic reactions but a highly specific signalling molecule acting both in the central and in the peripheral nervous systems under physiological conditions.[11–13] However, despite the progress made in understanding how H_2O_2 acts as a signalling molecule in the cell, its participation in redox-mediated survival signalling in retinal culture systems has not previously been investigated.

In the present study, we demonstrate for the first time that a transient increase in H_2O_2 occurs in retina-derived 661W cells when they are subjected to the stress of serum withdrawal. We propose that this oxidant burst, which is due at least in part to Nox2 activity, has two principle effects: upregulation of the AKT survival pathway and suppression of the apoptotic machinery. We demonstrate here that activation of the AKT survival pathway occurs via oxidation of the protein tyrosine phosphatase PTEN, which in turn upregulates the PI-3 (phosphatidylinositol-3-OH) kinase/AKT pathway. After 1-h serum withdrawal, H_2O_2 levels decline to basal levels, and we propose that this results in deactivation of survival pathways and activation of cell death effectors. In corroborative experiments, we demonstrate that maintaining H_2O_2 levels by addition of exogenous H_2O_2 increases survival of

serum-deprived 661W cells by enhancing and prolonging activation of the AKT survival pathway, and by delaying activation of cell death cascades. Furthermore, we demonstrate that H_2O_2 accumulation occurs in response to a variety of apoptotic stimuli, and this effect is observed in a second cell type, the retinal ganglion cell line RGC-5. Finally, we show that retinal explants upregulate p-AKT when treated with a sublethal dose of H_2O_2. These preliminary data suggest that H_2O_2 may also mediate a survival response in primary retinal cultures.

Results

Serum withdrawal induces a rapid and transient increase in H_2O_2 levels in 661W cone photoreceptors. To examine ROS production in response to apoptotic stimuli, we cultured 661W cone photoreceptor cells in the absence of trophic support. We observed a significant increase in intracellular H_2O_2 levels after 5 min of serum withdrawal, and this increase was sustained for up to 1 h (Figure 1a). Subsequently, H_2O_2 levels declined towards basal levels.

This increase in H_2O_2 levels was completely abrogated by the radical scavenger CR-6 (3,4-dihydro-6-hydroxy-7-methoxy-2,2-dimethyl-1(2*H*)-benzopyran)[14,17] (Figure 1b). Furthermore, H_2O_2 production was significantly reduced by the Nox inhibitor diphenyleneiodonium (DPI), suggesting a role for the Nox system in H_2O_2 generation. To further investigate the source of H_2O_2, we characterized expression of Nox family members in 661W cells. Immunoblotting analysis and semi-quantitative PCR revealed that only Nox2 and Nox4 are expressed in 661W cells. Suppression of Nox2 using small interfering RNA (siRNA) resulted in a significant decrease in H_2O_2 production in response to serum starvation compared to control samples (Figure 1c and d), suggesting that the oxidant burst is at least partially derived from Nox2 activity.

As H_2O_2 levels are rapidly and transiently increased in response to serum withdrawal, we hypothesized that it may mediate survival signalling. For this reason, we next sought to examine cell death in response to serum starvation in the presence of CR-6 and NAC, both antioxidants that scavenge H_2O_2. In Figure 1e, cell death upon serum starvation was significantly increased in samples pretreated with CR-6 and NAC. Furthermore, pretreatment with the Nox inhibitor, apocynin, significantly increased cell death compared to control samples (Figure 1e), demonstrating a role for H_2O_2 in cell survival. To confirm this, we quantified the number of apoptotic cells by annexin V labelling. Pretreatment with CR-6 increased the percentage of apoptotic cells from 4 ± 1 to $12 \pm 1\%$ (mean $\pm$ S.D.) (Figure 1f). These results demonstrate that removal of trophic support induces a rapid and transient increase in intracellular H_2O_2 levels and this H_2O_2 is partially generated by Nox2.

H_2O_2 accumulation in serum-deprived 661W cells promotes upregulation of the AKT pathway. Previous studies have demonstrated that the generation of H_2O_2 controls the activity of phosphatases, such as PTEN, regulating survival signalling.[18,19] To examine this theory in

our system, we examined PTEN oxidation in serum-starved 661Ws. In Figure 2a, the presence of the oxidized form of PTEN was evident 5 min after serum withdrawal, and pretreatment with CR-6 significantly reduced levels of this form of the protein. Since PTEN is a negative regulator of the PI-3 kinase/AKT survival pathway,[20,21] we propose that inactivation of PTEN by oxidation would allow increased AKT phosphorylation and subsequently, increased survival signalling. Serum deprivation resulted in a significant increase in p-AKT after just 5 min, and this was maintained for 30 min (Figure 2b). Thereafter, p-AKT levels declined towards basal levels. This result shows that AKT phosphorylation directly correlates with H_2O_2 levels in the cell. To confirm that H_2O_2 regulates AKT phosphorylation, we compared AKT phosphorylation status in the presence or absence of CR-6. As expected, pretreatment with CR-6 prevented an increase in p-AKT levels in serum-deprived 661W cells (Figure 2c).

To confirm an anti-apoptotic role for AKT, we pre-incubated 661W cells with the PI-3 kinase inhibitor LY294002 for 1 h prior to serum withdrawal. Under these conditions, we observed a substantial increase in cell death after 24 h as determined by propidium iodide (PI) uptake (Figure 2d). Inhibition of the AKT pathway increased cell death to $34 \pm 2\%$ (mean $\pm$ S.D.). While we propose that H_2O_2 acts upstream to mediate activation of the PI-3 kinase pathway, other reports have suggested that PI-3 kinase can regulate production of H_2O_2.[22,23] In Figure 2e, we show that pretreatment with LY294002 does not prevent the increase in H_2O_2 levels after 15-min serum withdrawal, suggesting that H_2O_2 generation lies upstream of the AKT pathway. In summary, serum starvation results in a burst of H_2O_2, which correlates with oxidation of PTEN and activation of the AKT pathway. Scavenging H_2O_2 with CR-6 results in decreased cell survival, and decreased phosphorylation of AKT. We therefore propose that H_2O_2 acts as a pro-survival signalling molecule, possibly by inhibition of PTEN activity.

Detection of early apoptotic events following the decline of the H_2O_2 burst. Downregulation of the AKT pathway following the decline of H_2O_2 levels suggested that early apoptotic events might be occurring at this stage. Mitochondrial permeabilization is an early apoptotic event and precedes the activation of cell death cascades.[24] JC-1 (5,5′,6,6′-tetrachloro-1,1′,3,3′-tetrabenzimidazolecarbocyanine iodide) was used to examine mitochondrial membrane potential ($\Delta\Psi_m$) in serum-deprived 661W cells. Figure 3a shows that 1-h serum starvation produces a substantial shift in the fluorescence emission, indicating a decrease of $\Delta\Psi_m$. After 4-h serum withdrawal, it was completely restored.

Disruption of mitochondrial functions leads to superoxide overproduction in the mitochondria. In the eye, both nitric oxide and superoxide anions are known to mediate retinal degeneration *in vivo*.[25] Hydroethidine (DHE) was used to monitor superoxide anion formation. Increased superoxide formation was not detected until 1 h after serum withdrawal (Figure 3b), corresponding with $\Delta\Psi_m$ collapse. Parallel monitoring of nitric oxide levels with DAF-FM (4-amino-5-methylamino-2′,7′-difluorescein) showed the same pattern
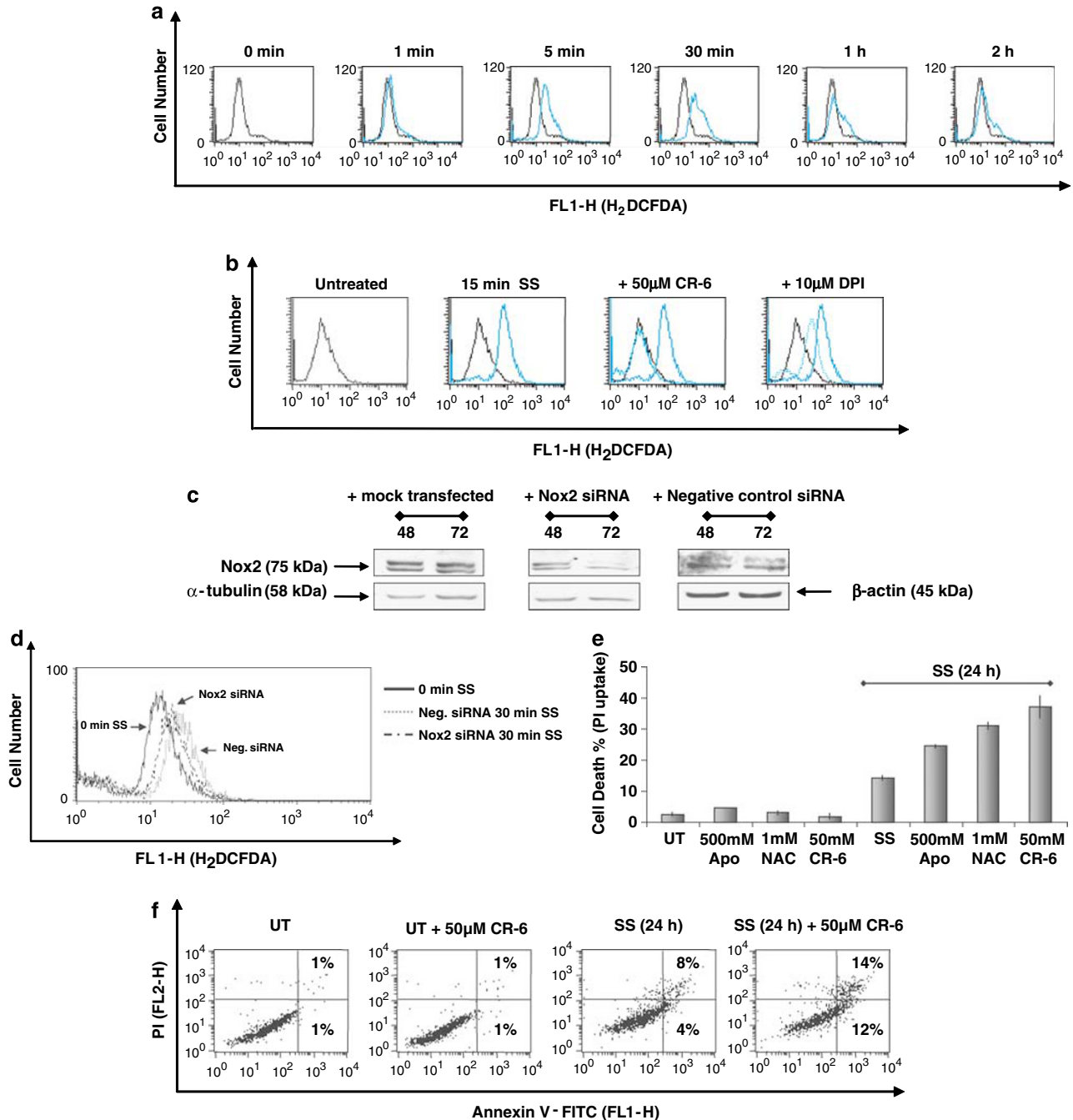
Figure 1 Serum starvation induces a rapid and transient production of hydrogen peroxide in 661W cone photoreceptors. (**a**) Hydrogen peroxide was detected by flow cytometry using the probe H_2DCFDA in 661W cells following serum withdrawal. The dark and light lines in the histograms correspond to control cells and serum-deprived 661W cells, respectively. (**b**) The NADPH oxidase inhibitor DPI and the radical scavenger CR-6 prevent the increase in hydrogen peroxide concentration in serum-free 661W cells. Cells were pre-incubated with 10 μM DPI and 50 μM CR-6 for 1 h and 15 min, respectively, before serum withdrawal. Hydrogen peroxide levels were measured 15 min after serum deprivation. Negative and positive controls (untreated and serum-deprived (SS) 661W cells) are represented with a dark and a light line, respectively. DPI- and CR-6-treated cells are shown by a dotted line. (**c**) Analysis of Nox2 expression in mock and Nox2 siRNA-transfected 661W cells. Total lysates were analysed by immunoblotting using an antibody against Nox2 and α-tubulin (loading control). (**d**) FACS analysis of hydrogen peroxide production in mock and Nox2 siRNA-transfected 661W cells. (**e**) Cells pretreated with CR-6, NAC or apocynin (Apo) were maintained in complete media or serum-starved for 24 h. Cell death was quantified by flow cytometry using PI. Results are mean ± S.D. (standard deviation) ($n = 3$). Results are representative of three independent experiments. (**f**) Apoptosis was determined by annexin V *versus* PI staining of 661W cells cultured in serum-free medium for 24 h. Annexin V^+/PI^- population (early stages of apoptosis) is represented in the lower right quadrant, whereas annexin V^+/PI^+ (late apoptotic or secondary necrotic cells) is shown in the upper right quadrant. All results are representative of at least three independent experiments

(Figure 3b). Elevated cytosolic Ca^{2+} also plays a role in photoreceptor apoptosis.[25,26] Analysis of intracellular Ca^{2+} using Fluo3-AM (fluo-3-acetoxymethyl ester) showed a shift in the fluorescence peak after 2-h treatment, indicating an increase in the levels of free cytoplasmic Ca^{2+} (Figure 3c). Overall, these results demonstrate that early apoptotic events
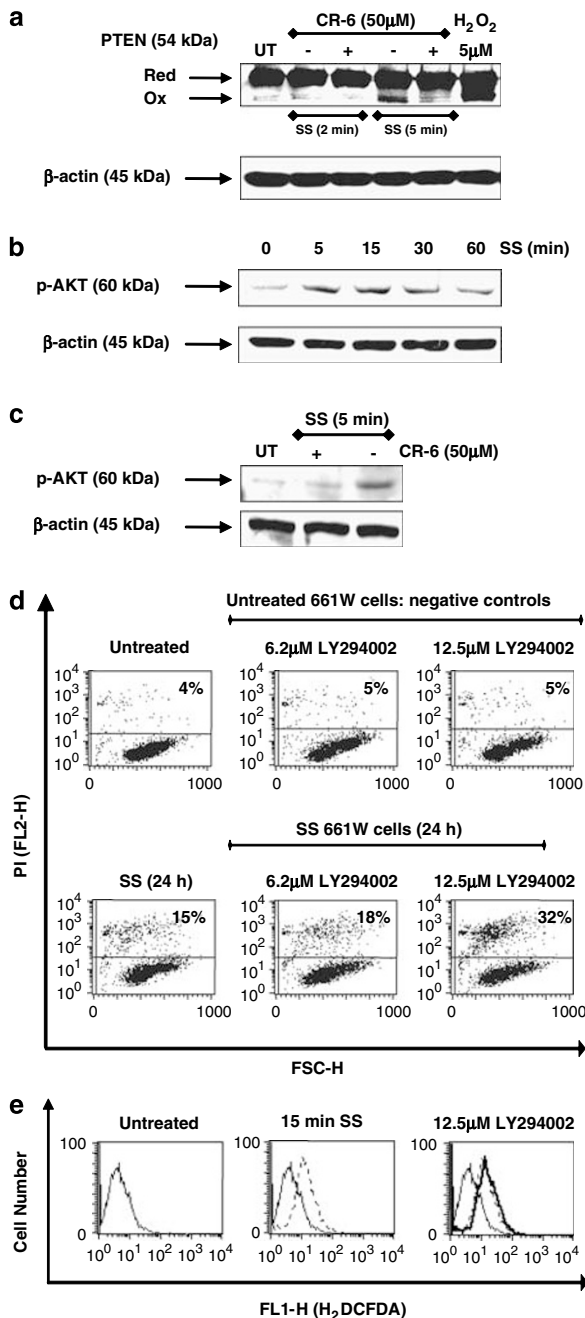
Figure 2 Hydrogen peroxide burst triggers activation of p-AKT survival pathway in serum-deprived 661W cells. (**a**) Oxidation of PTEN in 661W cells following 1- and 5-min serum withdrawal was examined by western blot analysis of whole cell lysates. Lysates from cells treated with 5 μM H_2O_2 was used as a positive control for PTEN oxidation. (**b**) Whole lysates from cells starved for indicated times were subjected to western blot with an antibody against phospho-Thr 308 AKT. (**c**) p-AKT levels were compared in 661W cells treated with or without 50 μM CR-6 after 5-min serum deprivation. Blots were probed with β-actin to verify equal loading. (**d**) 661W cells were incubated for 1 h with 6.25 and 12.5 μM LY294002 before serum withdrawal. Cell death was determined by flow cytometry using PI after 24 h treatment. Results are representative of three independent experiments. (**e**) H_2O_2 production was measured by flow cytometry using the probe H_2DCFDA. Cells were pretreated with 12.5 μM LY294002 and serum-starved for 15 min before analysis. Negative and positive controls (untreated and serum-deprived 661W cells) are represented with a continuous and a dotted line, respectively. Inhibitor pretreated cells are shown by a thick line. All experiments were repeated three times with comparable results

are detectable following the decline in the H_2O_2 burst. This strengthens our hypothesis that H_2O_2 acts rapidly to promote cell survival in response to serum starvation in our system.

Activation of apoptotic proteases following decline of the oxidant burst. Previously, we demonstrated parallel activation of caspases and calpains in 661W cells following 24-h serum depletion.[26] Yet mitochondrial permeabilization occurs after 1 h of serum withdrawal. Therefore, we investigated whether caspase activation occurs at an earlier time point than previously demonstrated. Figure 4a shows that caspase-3 is active after 2-h serum deprivation. Moreover, immunoblotting for the caspase-3 substrate PARP (poly(ADP-ribose)polymerase**)**, demonstrated that PARP was also cleaved at this time point (Figure 4b).

Calpains are calcium-dependent proteases, which undergo autocleavage and become active following an increase in Ca^{2+}. Consistent with increased levels of free cytoplasmic Ca^{2+} observed following 2-h serum deprivation (Figure 3c), calpain cleavage was clearly evident at the same time point (Figure 4c). Besides caspases and calpains, endolysosomal cathepsin D also plays an important role both in *in vitro* and *in vivo* models of retinal apoptosis.[27,28] Figure 4d shows cathepsin D processing from its 52-kDa inactive form to its 32-kDa mature isoform after 2 h of serum starvation. To further confirm that apoptosis is occurring within hours after initiation of serum starvation, we measured apoptosis using fluorescein isothiocyanate (FITC)-conjugated annexin V. Figure 4e shows that after 4-h serum deprivation, the percentage of annexin V-positive cells increased from 2 to 8%. These data indicate that activation of apoptotic effectors and apoptosis is evident as early as 2 h after serum withdrawal in 661W cells.

Sublethal doses of H_2O_2 increase cell survival. On the basis of time course of H_2O_2 burst and initiation of apoptotic events, we propose that levels of H_2O_2 must first decline before death effectors can become active. To investigate this hypothesis, we exogenously added H_2O_2 to serum-deprived 661W cells and examined cell viability and PARP cleavage. Figure 5a shows the susceptibility of 661W cells to H_2O_2 in a concentration-dependent manner in the presence and absence of serum over 24 h. Concentrations up to 200 μM were not toxic under normal conditions, but following serum withdrawal H_2O_2 began to show toxic effects at 50 μM. However, Figure 5b shows that following 1-h serum withdrawal, addition of 25 μM H_2O_2 can significantly increase viability of serum-deprived 661W cells. Lower concentrations of H_2O_2 did not provide protection, while higher concentrations showed either no effect or increased cell death.

We next investigated downstream effects in response to exogenous H_2O_2 addition. We examined p-AKT levels and PARP cleavage and compared those to serum-deprived 661W cells not supplemented with H_2O_2 (Figure 5c). Addition of 25 μM H_2O_2 after 1-h serum withdrawal significantly increased p-AKT levels. Accordingly, PARP cleavage was not detected after 2- or 4-h serum deprivation in 661W cells supplemented with H_2O_2 (Figure 5d). We then examined the
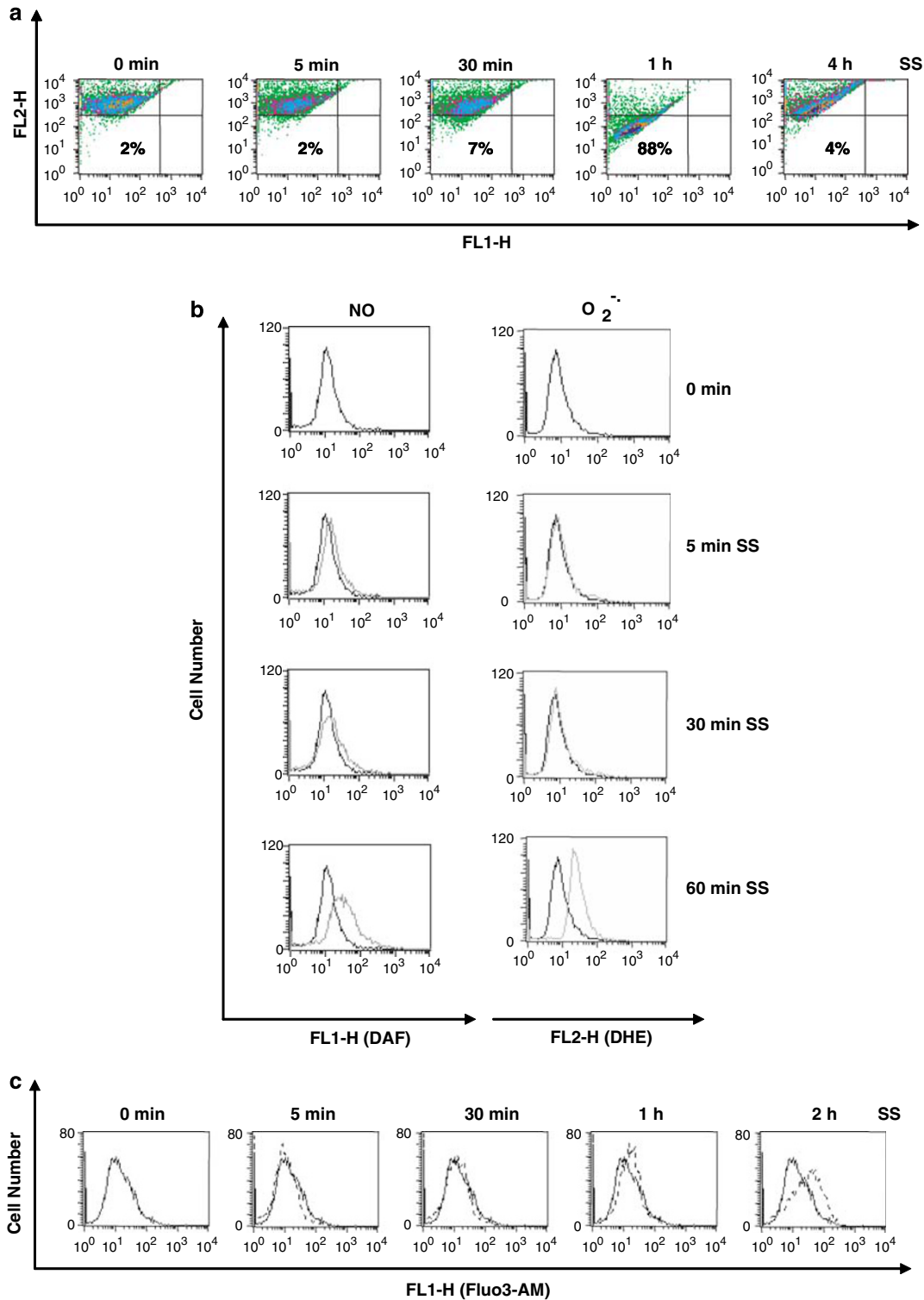
Figure 3 Biochemical study of early apoptotic events. (**a–c**) Flow cytometry analysis. (**a**) $\Delta\Psi_m$ was measured using the fluorescent probe JC-1 prior to serum starvation (0 min) and following the indicated times of serum withdrawal. (**b**) Following serum starvation of 661W cells for 5, 30 and 60 min, nitric oxide and superoxide levels were measured with DAF and DHE probes, respectively. Untreated and serum-deprived 661W cells are represented with a dark and a light line, respectively. (**c**) Intracellular Ca^{2+} levels were monitored in 661W cells cultured in serum-free medium for indicated times using the Fluo3-AM probe. Results are representative of three experiments, with duplicate samples in each experiment

Figure 4 Biochemical study of apoptotic proteases. (**a**) Caspase-3 activity was assessed by cleavage of the colorimetric peptide substrate Ac-DEVD-*p*NA (Abs 405 nm) in 661W lysates that had been serum-starved f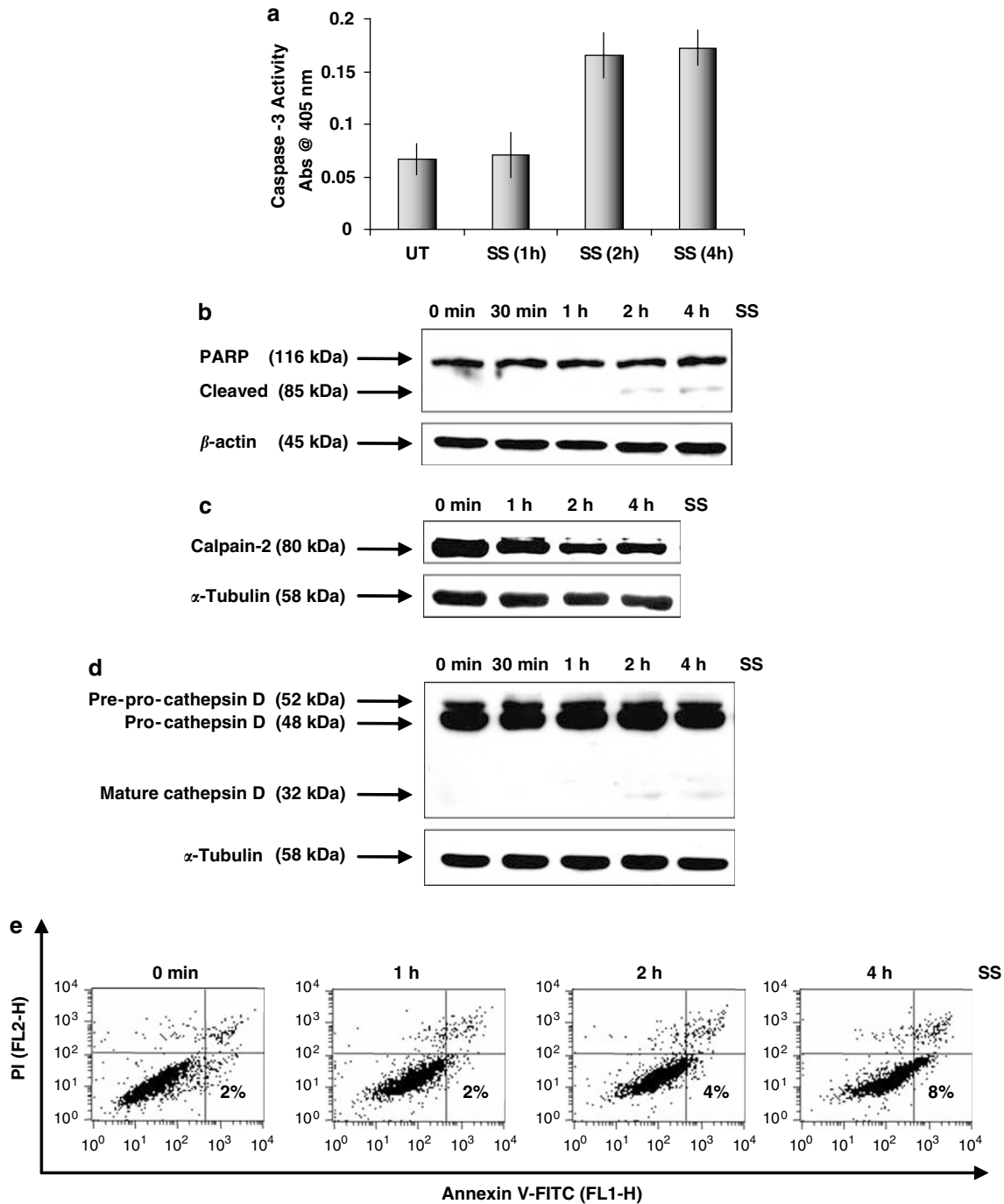or 1, 2 and 4 h. Data represent mean ± S.D. (*n* = 3). (**b**) Whole lysates from 661W cells starved for indicated times were subjected to western blot with an antibody against PARP. (**c**) Calpain activity was analysed by western blotting following 1-, 2- and 4-h serum withdrawal. Decreased detection of the 80-kDa band indicates calpain-2 cleavage and activation. (**d**) Western blot analysis of cathepsin D in 661W cells cultured in serum-free medium for 30 min, 1, 2 and 4 h. *β*-Actin or *α*-tubulin were used as a loading control. (**e**) Apoptosis was determined by annexin V *versus* PI staining of 661W cells cultured in serum-free medium for 1, 2 and 4 h. All assays are representative of three experiments, with duplicate samples in each experiment

effects of high/low concentrations of H_2O_2 on PARP cleavage, and p-AKT levels (Figure 5e). Following serum withdrawal, 10 μM H_2O_2 did not prevent PARP cleavage while 200 μM H_2O_2 increased cleavage of the 116 kDa PARP band over control levels as expected (Figure 5e). These data correlate with results shown in Figure 5a. H_2O_2 also increased p-AKT levels at both concentrations tested. However, we have demonstrated 200 μM H_2O_2 is toxic under serum withdrawal conditions and this correlates with increased PARP cleavage following 4-h serum withdrawal (Figure 5e).
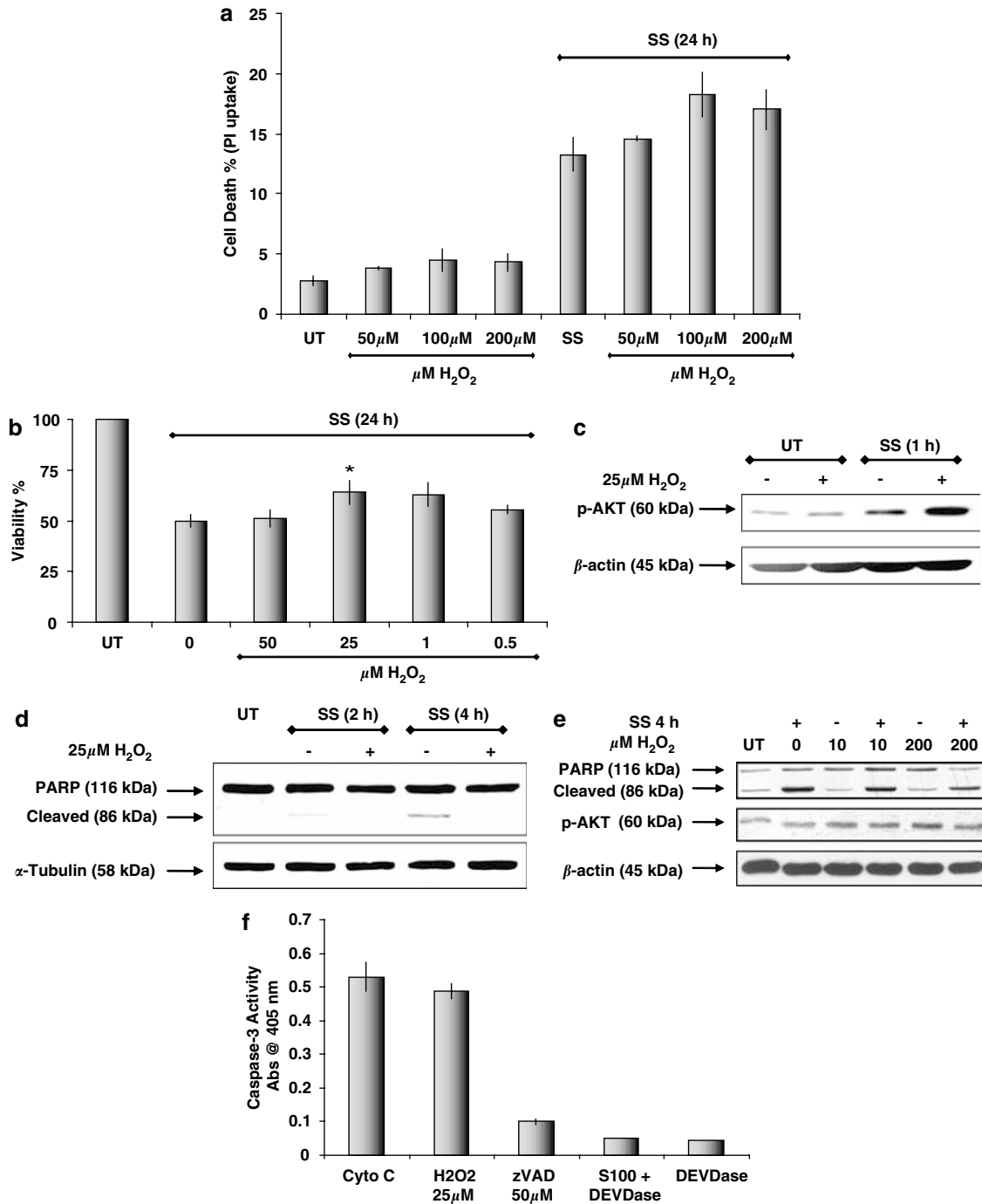
Figure 5 Exogenous addition of hydrogen peroxide increases cell survival in serum-deprived 661W cells. (**a**) 661W cells cultured in serum or serum-free medium for 1 h were treated with increasing concentrations of H_2O_2. Cells were maintained in culture for a further 23 h and cell death was determined by flow cytometry using PI uptake. Results are mean ± S.D. ($n = 3$). Results are representative of three independent experiments. (**b**) H_2O_2 was added to 661W cells that had been cultured in serum-free medium for 1 h. Cells were maintained in serum-free media for a further 23 h, and viable cells were quantified by crystal violet staining. Results represent the mean ± S.D. ($n = 3$), *$P < 0.05$. (**c**) Following serum withdrawal for 1 h, supplemented with or without 25 μM H_2O_2, whole cell lysates were obtained and resolved by SDS-PAGE. Blots were probed with phospho-AKT (Thr308) and β-actin as a loading control. (**d**) Following serum withdrawal for 2 and 4 h, supplemented with or without 25 μM H_2O_2, whole cell lysates were obtained and resolved by SDS-PAGE. Blots were probed with PARP antibody, and α-tubulin levels were used as a loading control. Results are representative of at least three independent experiments. (**e**) Western blot analysis following 4 h serum withdrawal, supplemented with or without 10 or 200 μM H_2O_2, whole cell lysates were obtained and resolved by SDS-PAGE. Blots were probed with PARP and phospho-AKT (308) antibody. β-actin levels were used as a loading control. Results are representative of three independent experiments. (**f**) Caspase-3 activity in 661W S-100 cytosol fractions was assessed by cleavage of the colorimetric peptide substrate Ac-DEVD-*p*NA (Abs 405 nm). Apoptosis was induced by addition of cytochrome *c* and dATP in samples that had or had not been pretreated with 25 μM H_2O_2 or 50 μM z-VAD-fmk for 1 h. S-100 cytosol without cytochrome *c* addition and substrate alone were used as controls. Data represent mean ± S.D. ($n = 3$)

To confirm that H_2O_2 was not directly acting on caspases to inhibit their activity, cell-free assays were performed in which caspase activity was measured in the presence and absence of H_2O_2, or the pan-caspase inhibitor z-VAD-fmk as a positive control. In samples pretreated with $25 \mu M$ H_2O_2, caspase activity was not inhibited following induction of apoptosis with cytochrome *c* compared to samples pretreated with zVAD (Figure 5f). On the basis of these data, we propose that prolonging the transient increase in H_2O_2 levels following serum starvation by exogenous addition of H_2O_2 enhances cell survival by increasing p-AKT levels and preventing the activation of cell death effectors.

Different apoptotic stimuli induce an early burst of H_2O_2 in 661W and RGC-5 cells. To investigate whether the H_2O_2 burst was a phenomenon exclusively associated with the removal of trophic support, we exposed 661W cells to other stress stimuli; namely the nitric oxide donor sodium nitroprusside (SNP); the tyrosine kinase inhibitor staurosporine (STS); the genotoxic agent etoposide (VP16) and UV radiation. Following 15-min exposure, all stimuli induced a substantial increase in H_2O_2 concentration, suggesting that the early oxidant burst is stimulus independent. Pretreatment with 1 mM NAC before stimulation prevented H_2O_2 accumulation in all cases (Figure 6a).

To determine whether H_2O_2 levels increase in response to stress in another cell type, we examined the response of the rat RGC-5 line to the same stimuli. As observed for 661W cells, H_2O_2 levels increased rapidly after initiation of stress in RGC-5 cells. Similarly, NAC prevented the oxidant burst in RGC-5 cells in response to all stimuli (Figure 6b). The effect of the H_2O_2 burst on cell survival was evaluated in 661W and RGC-5 cells (Figure 6c and d) by quantifying the percentage of apoptotic cells after stress in the presence or absence of NAC. Inhibition of H_2O_2 production with NAC increased the death rate in those cells that had been treated with an oxidative stress inducer but not VP16 or STS. Taken together, these results strengthen our hypothesis that the oxidant burst mediates cell survival signalling under stress conditions.

Exogenous H_2O_2 increase AKT levels in mouse retinal explant cultures. To investigate the possibility that H_2O_2 could promote cell survival via upregulation of the AKT pathway *in vitro/ex vivo*, we employed mouse retinal explant cultures. A previous publication demonstrated that $200 \mu M$ H_2O_2 is toxic to primary cultured mouse RGCs,[29] while $600 \mu M$ H_2O_2 is required to induce apoptosis in retinal explant cultures.[30] Therefore, we decided to examine a range of concentrations of H_2O_2 on retinal explants to determine a concentration that was not toxic and that could be used in further experiments. Figure 7a shows terminal deoxynucleotidyl transferase-mediated biotinylated UTP nick end labelling (TUNEL) staining of P10 mouse retinal explant sections subjected to increasing concentrations of H_2O_2 for 24 h. We found $50 \mu M$ H_2O_2 did not increase the number of TUNEL-positive nuclei in the outer nuclear layer (ONL) where photoreceptors are located or the ganglion cell layer (GCL) where RGCs are found, above untreated control levels over 24 h. However, 150, 300 and $600 \mu M$ H_2O_2 steadily

increased the number of TUNEL-positive nuclei in both the ONL and the GCL in a concentration-dependent manner over 24 h. Interestingly, this study shows an increased sensitivity of retinal explant cultures to H_2O_2 compared to the 661W photoreceptor cell line and the RGC-5 line (Figure 7b and c). Having established a concentration that was not toxic to retinal explant cultures, we next sought to examine if adding exogenous H_2O_2 could activate the AKT pathway as previously demonstrated in 661W cells (Figure 5b). Retinal explants were maintained in culture for 24 h before addition of H_2O_2 was carried out. Addition of $50 \mu M$ H_2O_2 to explant cultures resulted in a significant increase in p-AKT levels after 1 h (Figure 7d). The increase in p-AKT levels detected in retinal explants correlates with those observed in 661W cells (Figure 5c) and therefore may also be a survival mechanism employed by retinal explants. This is the first step towards validating our results in primary tissue.

Discussion

In the retina, previous studies have described a pro-apoptotic role for H_2O_2 in pathological conditions.[1,5,6] Furthermore, it is well established that exogenous addition of high doses of H_2O_2 triggers apoptosis.[31,32] It has been proposed, however, that the diverse outcomes of H_2O_2 production in the cell could be the result of subtle differences in the level and duration of the oxidant burst.[9] We hypothesize that the transient increase in H_2O_2 concentration observed in response to serum starvation of 661W cells (Figure 1a) is connected to cell survival rather than cell death. To address this, we inhibited H_2O_2 generation using CR-6 and analysed the effect on cell death (Figure 1b). We observed increased apoptosis in cells pretreated with CR-6, NAC and apopcynin (Figure 1e and f), suggesting that transient H_2O_2 accumulation serves as a survival signal. Partial inhibition of the oxidant burst with DPI suggested a link between the Nox system and H_2O_2 generation (Figure 1b). Studies using siRNA identified Nox2 as one of the enzymes responsible for H_2O_2 production (Figure 1c and d).

Once we had demonstrated that the H_2O_2 burst might be pro-survival, we sought to determine how this effect was mediated. H_2O_2 generation has been linked to the activity of the PI-3 kinase/AKT pathway.[22,23,33] One mechanism by which H_2O_2 can promote activation of survival pathways is by regulating the activity of protein tyrosine phosphatases, such as PTEN, through oxidation of catalytic cysteine residues.[19,34] Indeed, our results strongly suggest that stress-induced H_2O_2 production plays a key role in activating the PI-3 kinase/AKT pathway through the reversible oxidation and inactivation of PTEN (Figure 2a and b). The connection between the oxidant burst and the activation of AKT was reinforced by the studies with CR-6. Suppression of H_2O_2 production with CR-6 prevented AKT phosphorylation (Figure 2).

PI-3 kinase/AKT activation has been linked to inactivation of pro-apoptotic proteins. For example, AKT phosphorylation can inactivate BAD and caspase-9, suppressing apoptosis.[35,36] Therefore, we investigated if the decrease in p-AKT levels 1 h after serum withdrawal led to activation of cell death cascades. Analysis of mitochondrial membrane potential demonstrated $\Delta\Psi_m$ collapse after 1 h treatment (Figure 3a),
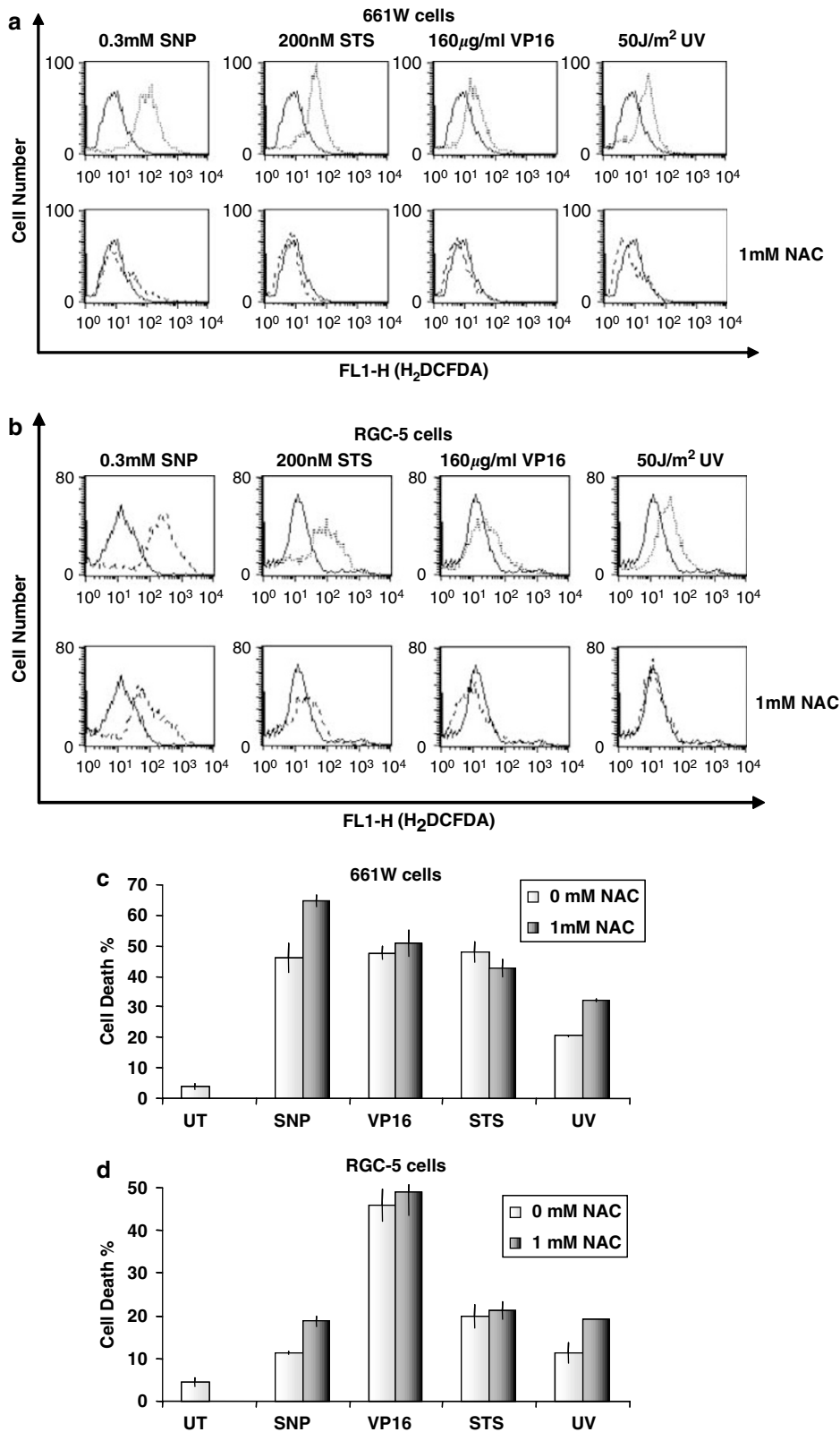
Figure 6 Hydrogen peroxide burst in 661W and RGC-5 cells is stimulus independent. 661W (**a**) and RGC-5 cells (**b**) were treated with SNP (0.3 mM), STS (200 nM), VP16 (160 μg/ml) and UV radiation (50 J/m^2) in the presence or absence of NAC. After 15 min, hydrogen peroxide levels were compared to untreated cells (continuous line) using the fluorescent probe H$_2$DCFDA. Results are representative of at least three independent experiments. Cell death was quantified after 24 h in 661W (**c**) and RGC-5 cells (**d**) by flow cytometry using PI. Results are mean $\pm$ S.D. ($n = 3$)

Figure 7 Sublethal dose of H_2O_2 increases p-AKT levels in mouse retinal explant cultures. (**a**) TUNEL staining of mouse retinal explants treated with increasi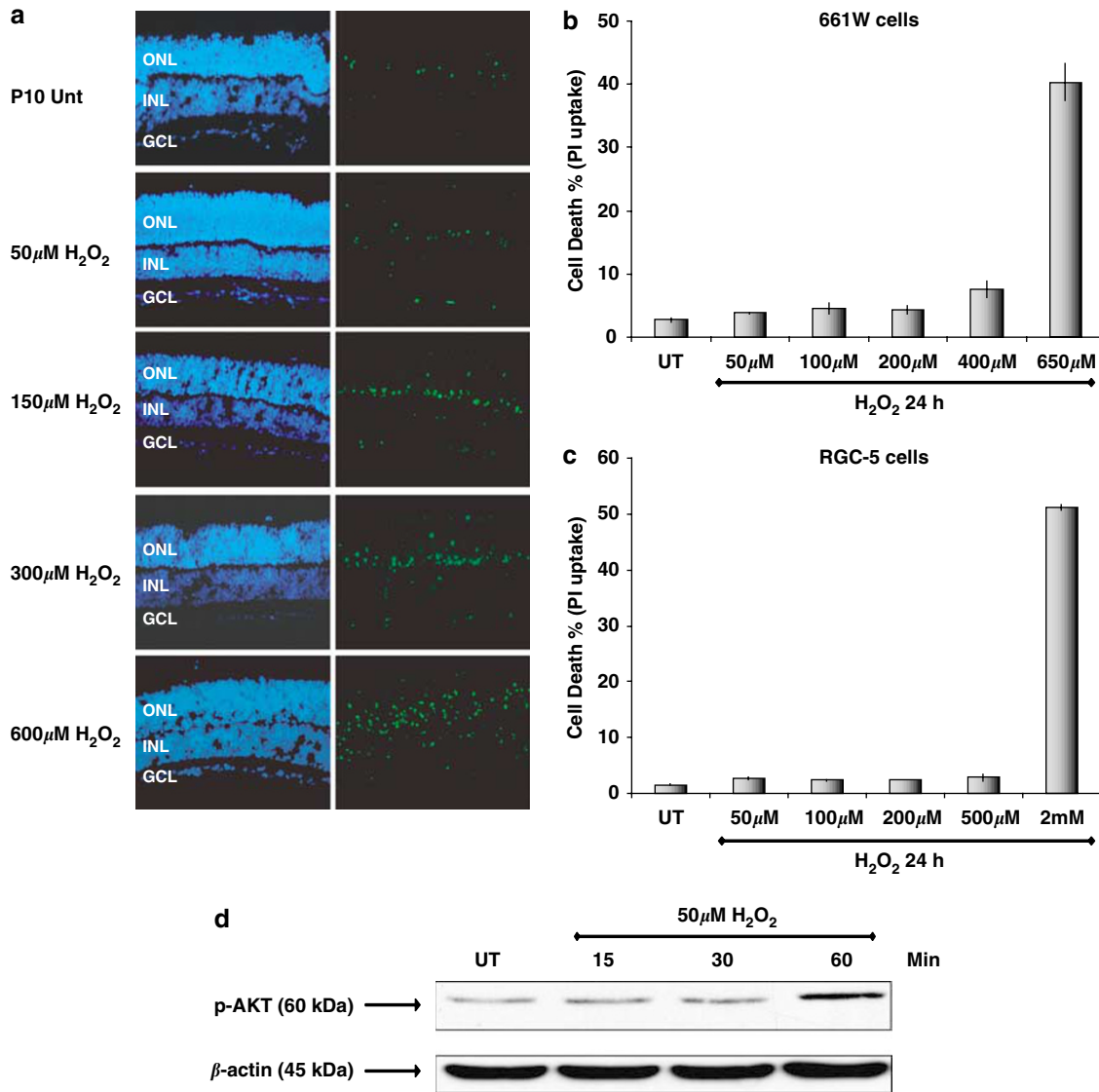ng concentrations of H_2O_2 for 24 h. Hoechst-stained nuclei of retinal explants are also shown. (**b**) 661W cells and (**c**) RGC-5 cells treated with increasing concentrations of H_2O_2. Cell death was determined by flow cytometry using PI uptake after 24 h treatment. Results are mean ± S.D. (standard deviation) $n = 3$. Results are representative of three independent experiments. (**d**) Western blot analysis of p-AKT in retinal explants untreated (UT) and treated with 50 μM H_2O_2 for the indicated times. β-actin was used as a loading control. Results are representative of at least three independent experiments

and activation of caspase-3 2 h after treatment (Figure 4a and b). Only after decline of p-AKT levels, did we observe an increase in superoxide, nitric oxide and cytoplasmatic Ca^{2+} concentration (Figure 3b and c). Therefore, elevated nitric oxide levels following 1-h serum deprivation might be responsible for mitochondrial dysfunction, increased production of superoxide and the activation of cell death mechanisms.[37]

Activation of the apoptotic machinery following the drop in the pro-survival pathways led us to question when proteases become activated in this model. Previous studies by our laboratory demonstrated that photoreceptor apoptosis involves the participation of multiple death pathways,[27] including calpains and caspases.[26] The present study corroborates previous observations but, additionally,

demonstrates the activation of proteases as early as 2 h after initiation of serum starvation (Figure 4). We also observed that cathepsin D participates in serum withdrawal-induced apoptosis in 661W cells 2 h after treatment correlating with caspase and calpain activation (Figure 4d). These results highlight the complexity of the apoptotic machinery in photoreceptor cells. However, despite the multiplicity of death pathways, we propose that their activity is regulated, at least in part, by the initial oxidant burst.

To confirm a role for H_2O_2 in mediating survival, we added a sublethal concentration of H_2O_2 to serum-deprived 661W cells. Wang et al.[38] showed that AKT is activated in response to submillimolar concentrations of H_2O_2 in several cell systems, whereas preconditioning with low concentrations of H_2O_2 enhances resistance of PC12 cells to apoptosis.[39,40]

In agreement with previous observations and with our hypothesis, addition of 25 μM H_2O_2 to serum-deprived 661W cells significantly increased cell survival by enhancement of p-AKT levels and prevention of PARP cleavage (Figure 5b and d). We also demonstrated that increased survival and prevention of PARP cleavage was not due to direct inhibition of capase-3 activity by H_2O_2 (Figure 5f). H_2O_2 concentrations higher than 25 μM either showed similar effects or increased cell death, while lower concentrations did not protect against cell death (Figure 5e). H_2O_2 was added 1 h after serum withdrawal, to boost peroxide concentration at the point where it begins to decline towards basal levels, and before activation of the apoptotic cascades. Following 2-h serum starvation, supplementation with 25 μM H_2O_2 did not enhance cell survival. Therefore, it appears that H_2O_2 cannot halt the process once it has been initiated.

We appreciate that the window of efficacy is narrow and that different concentrations of H_2O_2 might be required to elicit the same effects in primary explant cultures *versus* cell lines. Indeed, we demonstrate that while 600 μM H_2O_2 induces significant apoptosis in photoreceptors of retinal explants (similar to 661W cells), survival effects are mediated by the slightly higher concentration of 50 μM H_2O_2. This suggests that while the principle of H_2O_2 as a survival mediator may carry over from cell lines to explant cultures the effective range appears to be different.

Finally, our study demonstrated that an oxidant burst occurs in response to several different apoptotic stimuli, and was also observed in a second cell type the RGC line (Figure 6). A variety of apoptotic inducers, including SNP, UV, STS and VP16, provoked a rapid and transient increase in H_2O_2 levels. However, the H_2O_2 pro-survival role seems to be associated only with oxidative stress-related stimuli, SNP and UV, and not with STS and VP16. Although STS elicited a H_2O_2 burst, it is a protein kinase inhibitor; therefore, a survival signal evoked by H_2O_2 mediated by kinases may not be functional in STS-treated cells. Furthermore, treatment with topoisomerase II inhibitor VP16 produced a burst of H_2O_2 that did not appear to be pro-survival. The reason for this remains unclear but it does suggest that H_2O_2 is acting as a survival signal only in certain cases (Figure 8).

In this study, we present the novel finding that two retinal cell lines, treated with various apoptotic stimuli produce a rapid and transient increase in H_2O_2, which acts as a pro-survival signal, by oxidizing PTEN and increasing p-AKT. Therefore, we hypothesize that H_2O_2 can be a pro-survival molecule in retinal cell lines and preliminary data suggest that H_2O_2 may have a similar role in photoreceptors of retinal explant cultures. However, further work is required to establish a model of endogenous H_2O_2 production in this system.

Materials and Methods

Drugs, reagents and antibodies. H_2O_2, DPI (diphenyleneiodonium), hexamethylpararosaniline chloride (crystal violet), cytochrome *c*, dATP, SNP, STS, VP16 and *N*-acetyl-L-cysteine (NAC) were purchased from Sigma (Dublin, Ireland). The pan-caspase inhibitor z-VAD-fmk was purchased from Bachem (Saffron Walden, UK). Apocynin was obtained from Calbiochem (Nottingham, UK). The synthesis of CR-6 has been described elsewhere.[14] Cell Signalling Technology (Hertfordshire, UK) provided the following antibodies: PTEN (no. 9552), PARP
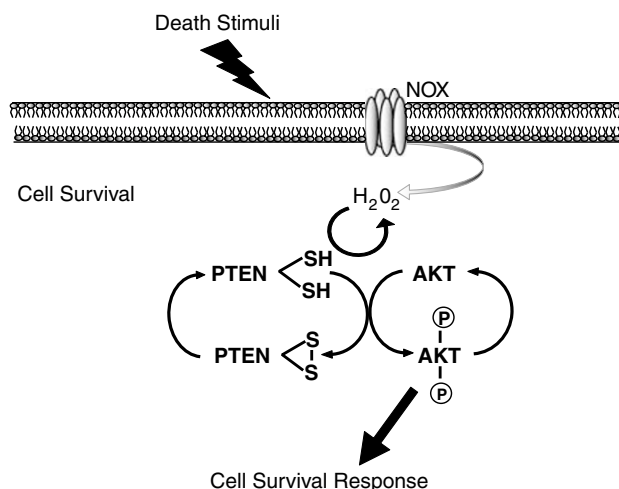

Figure 8 Schematic diagram illustrating the proposed survival role of H_2O_2 in 661W photoreceptor cells. Serum starvation of 661W cells results in a rapid and transient burst of H_2O_2. Nox2 has been identified as one of the enzymes responsible for H_2O_2 production. We propose that, once generated, H_2O_2, promotes activation of the AKT survival pathway by regulating the activity of the protein tyrosine phosphatase, PTEN. H_2O_2 reversibly oxidizes and inactivates PTEN, which in turn stimulates AKT phosphorylation and promotes survival. We suggest that return of H_2O_2 to basal level results in activation of PTEN, followed by decreased AKT phosphorylation and cell survival

(no. 9542) and phospho-AKT (Thr308) (no. 9275). Nox2 antibody (anti-gp91-phox, no. 07-024) was obtained from Upstate (Dublin, Ireland). Calpain-2 antibody (no. 208755) was purchased from Calbiochem. Cathepsin D antibody (no. sc-6486) was obtained from Santa Cruz Biotechnology (Santa Cruz, CA, USA) and α-tubulin (no. T-5168) and β-actin (no. A-5441) from Sigma. Peroxidase-conjugated anti-rabbit and anti-mouse secondary antibodies were obtained from Dako (Glostrup, Denmark). Caspase-3 chromogenic substrate Ac-DEVD-*p*NA (acetyl-Asp-Glu-Val-Asp-*p*-nitroanilide) was provided by Alexis Biochemicals (Läufefingen, Switzerland). The PI-3 kinase inhibitor LY294002 was obtained from Calbiochem.

Cell culture. The 661W photoreceptor cell line was generously provided by Dr. Muayyad Al-Ubaidi (Department of Cell Biology, University of Oklahoma Health Sciences Center, Oklahoma City, OK, USA). The RGC-5 line was a kind gift from Dr. Neeraj Agarwal (Fort Worth, TX, USA). These cells were routinely grown in Dulbecco's modified Eagle's medium supplemented with 10% heat-inactivated fetal calf serum (both from Sigma) and 1% penicillin/streptomycin, at 37°C in a humidified atmosphere with 5% CO_2. To induce apoptosis, 75 000 cells per well were seeded onto tissue culture six-well plates (NalgeNUNC International, Hereford, UK) and allowed to attach for 24 h. Cells were then washed twice with phosphate-buffered saline (PBS, pH 7.4), and serum-free medium was added to each well. Pretreatment with CR-6 was performed for 15 min, while pretreatment with NAC and apocynin was performed for 1 h, respectively, at 37°C. H_2O_2 was added to a final concentration of 25 μM unless otherwise indicated after 1-h incubation in serum-free medium. After incubation for the indicated times, cells were detached with a trypsin-EDTA solution (Sigma) and, together with their supernatants, were washed once with ice-cold PBS.

Measurement of H_2O_2 levels. H_2O_2 production was monitored as previously described.[15] Briefly, following treatment, 100 μM H$_2$DCFDA (2′,7′-dichlorodihydrofluorescein diacetate; Molecular Probes, Leiden, The Netherlands) was added and samples were incubated for 15 min at 37°C before analysis on a FACScan flow cytometer (Becton Dickinson, Oxford, UK). H_2O_2 production was measured at FL-1 (530 nm) with excitation at 488 nm. CellQuest software (Becton Dickinson) was used for data analysis and 10 000 events per sample were acquired.

siRNA transfection. Cells (661W) were plated 24 h before transfection in a six-well plate (12 000 cells per well). The transfection reagent, RNAifect (Qiagen,

Crawley, UK), was used according to the manufacturer's protocol to transfect negative control siRNA (no.1027310; Qiagen) or Silencer® pre-designed siRNA against murine Nox2 (ID 160437, 5′-GCCUUGGCUGAAACUCUCAtt-3′; Ambion, Warrington, UK) at a final concentration of 100 nM. Assays were performed 48 and 72 h post-transfection.

Cell death measurements: PI uptake and annexin V staining. Cell viability was assessed by PI (Sigma) uptake on a FACScan flow cytometer at 590 nm (FL-2). The criteria for cell death were based on changes in the light scattering properties of dead cells due to shrinkage and increased granularity as well as increased permeability to PI. Following treatments, cells were collected as described above, washed once with ice-cold PBS and resuspended to a final concentration of 1×10^5 cells/ml. PI was added to a final concentration of 50 μg/ml and samples were immediately analysed. Double staining with FITC-conjugated annexin V and PI was performed for quantification of apoptotic cells. Cells were harvested, washed once with ice-cold PBS and resuspended in 100 μl of Ca^{2+}-binding buffer (10 mM HEPES pH 7.4, 140 mM NaCl, 2.5 mM CaCl$_2$) containing 1 : 10 annexin V-FITC solution (IQ Products, Groningen, The Netherlands). After 15-min incubation in the dark at a room temperature (RT) of 20°C, 400 μl of binding buffer with PI was added to each sample immediately before flow cytometry analysis. Samples were analysed in a FACScan flow cytometer using the software CellQuest for data analysis. A total of 10 000 events per sample were acquired.

Western blotting. Cells (8×10^5 per flask) were plated in 75 cm^2 flasks (Sarstedt AG & Co.) and allowed to attach overnight. Apoptosis was induced by replacing the routine medium with serum-free medium. After the appropriate incubation times, whole cell extracts were obtained and resolved by denaturing sodium dodecyl sulphate-polyacrylamide gel electrophoresis (SDS-PAGE). Briefly, cells were scraped and, together with supernatant, washed twice with ice-cold PBS followed by resuspension in cell lysis buffer (50 mM Tris-HCl pH 7.4, 150 mM NaCl, 1 mM Na$_3$VO$_4$, 1 mM NaF, 1 mM EGTA, 1% Nonidet P-40 (NP40), 0.25% sodium deoxycholate) containing the cocktail of protein inhibitors antipain (1 μg/ml), aprotinin (1 μg/ml), chymostatin (1 μg/ml), leupeptin (0.1 μg/ml), pepstatin (1 μg/ml) and 0.2 mM AEBSF. After incubation on ice for 20 min, debris was removed by centrifugation (10 000 × *g*) at 4°C and protein concentration was quantified by Bio-Rad (Hemel Hempstead, UK) assay, using bovine serum albumin as a standard. Proteins (20–40 μg) were diluted in 2 × sample buffer (10% SDS, 100 mM dithiothreitol (DTT), glycerol, bromophenol blue, Tris-HCl) and resolved on 6–12% SDS-PAGE gels. In the case of non-reducing SDS-PAGE, cell lysates were prepared with the above-described lysis buffer containing 50 mM Tris-HCl pH 8.0 and 50 nM *N*-ethylmaleimide to block free sulphhydryl groups. Gels were run in the absence of DTT. Proteins were transferred onto nitrocellulose membranes (Schleicher & Schuell, Whatman, Dassel, Germany) and blots were blocked with 5% (w/v) non-fat dry milk in Tris-buffered saline/0.1% Tween-20 (TBS/T), for 1 h at RT. Membranes were incubated at 4°C overnight, with the appropriate dilution of primary antibody (1 : 400 anti-cathepsin D, 1 : 500 PTEN and p-AKT, 1 : 1000 all others). After three 5-min washes with TBS/T, blots were incubated with the corresponding peroxidase-conjugated secondary antibody (dilution 1 : 1000) for 1 h at RT. They were then washed again three times with TBS/T, rinsed briefly with PBS and developed with the enhanced chemiluminescence reagents (ECL; Amersham Biosciences, Buckinghamshire, UK). Detection of α-tubulin or β-actin (both 1 : 5000) was used as a control for equal loading of protein.

Analysis of nitric oxide levels. Nitric oxide levels were quantified using the probe DAF-FMMolecular Probes). After trypsinization, cells were washed once with ice-cold PBS and resuspended in 200 μl of fresh buffer containing 10 μM DAF-FM. After 30-min incubation in the dark at 37°C, cells were washed in PBS to remove excess of probe. Fresh buffer was added and cells were incubated for an additional 15 min at 37°C. Fluorescence was measured in a FACScan flow cytometer FL-1 (515 nm) with excitation at 495 nm. A total of 10 000 events per sample were acquired.

Analysis of superoxide anion generation. Measurement of superoxide anion levels was carried out as previously described.[16] Briefly, cells were loaded with 10 μM DHE (Molecular Probes) for 15 min at 37°C. Superoxide anion oxidizes DHE intracellularly to produce ethidium bromide, which fluoresces upon interaction with DNA. Fluorescence due to ethidium bromide was monitored in a Becton Dickinson FACScan flow cytometer with excitation and emission at 488 and 590 nm,

respectively. CellQuest software was used for data analysis, and 10 000 events per sample were acquired.

Analysis of mitochondrial membrane depolarization. Mitochondrial membrane depolarization was analysed using the probe JC-1 (Molecular Probes). Cells were washed twice with ice-cold PBS before incubation with JC-1 (5 μg/ml) in darkness for 15 min at 37°C. At high $\Delta\Psi_m$, JC-1 forms J-aggregates, which fluoresce at 590 nm (measured in FL-2). At least 10 000 events per sample were acquired, using FACScan flow cytometer and CellQuest software.

Measurement of cytosolic-free Ca^{2+} levels. Cytosolic Ca^{2+} levels were determined using the intracellular Ca^{2+} probe, Fluo3-AM (Molecular Probes), which binds Ca^{2+} with a 1 : 1 stoichiometry. After trypsinization, cells were washed once with PBS and resuspended in fresh buffer. Cells were incubated in the darkness with Fluo-3 (250 nM) for 30 min at 37°C. Fluorescence was measured at FL-1 (530 nm) in a Becton Dickinson FACScan flow cytometer with excitation at 488 nm. At least 10 000 events per sample were acquired.

Caspase activity assay. Pellets from 8×10^5 untreated or serum-deprived 661W cells were resuspended in 50–100 μl chilled lysis buffer (50 mM HEPES pH 7.4, 100 mM NaCl, 0.1% 3-[(3-cholamidopropyl)dimethylammonio]-1-propanesulphonate, 1 mM DTT, 100 μM EDTA and 0.1% NP40) and incubated on ice for 10 min. Following a 20-s sonication, cell lysates were centrifuged at 4°C for 10 min (10 000 × *g*). An equal quantity of protein (50 μg) was loaded onto each well of a microtitre plate and the final volume was made up to 90 μl with assay buffer (as lysis buffer, minus 1% NP40). The reaction was initiated by addition of caspase-3-*p*NA substrate to a final concentration of 200 μM, from a 10 mM stock solution in dimethyl sulphoxide. After 1-, 2- and 4-h incubation at 37°C, cleavage of the peptide substrate DEVD-*p*NA was monitored by liberation of the chromogenic *p*NA in a SpectraMax-340 plate reader (Molecular Devices, Menlo Park, CA) by measuring absorption at 405 nm.

Preparation of cell-free extracts and cell-free reactions. Cell-free extracts were prepared from 661W cells as follows: cells were plated and incubated overnight. Cells were then scraped, washed in PBS, resuspended in 150 μl of cell extraction buffer (CEB) and transferred to a 2 ml dounce homogenizer (CEB; 20 mM HEPES-KOH, pH 7.5, 10 mM KCl, 1.5 mM MgCl$_2$, 1 mM EDTA, 1 mM EGTA, 1 mM DTT, 100 μM AEBSF, 10 mg/ml leupeptin, 2 mg/ml aprotinin). Cells were incubated for 15 min on ice, disrupted with 20 strokes of the pestle and incubated on ice for another 15 min. Lysates were centrifuged at 14 000 r.p.m. for 15 min at 4°C. The supernatant was then removed and further centrifuged at 100 000 × *g* for 1 h to obtain S-100 cytosols. The total amount of protein was determined by Bio-Rad protein assay (Bio-Rad), as previously. For cell-free reactions, 60 μg of protein was diluted to a final volume of 90 μl in caspase activity assay buffer per well of a microtitre plate. Samples were then incubated with either 25 μM H$_2$O$_2$ or 50 μM z-VAD-fmk for 1 h at RT. Apoptosis was induced by addition of bovine heart cytochrome *c* and dATP at final concentrations of 50 mg/ml and 1 mM, respectively. Samples were then incubated at 37°C for 1 h to initiate apoptosis before analysis of caspase-3 activity, as previously described.

Viability assay: crystal violet assay. Following treatment, cells were fixed with 96% ethanol for 10 min. Then, cells were stained with a 0.05% crystal violet solution in 20% ethanol for 30-min. After three washes with H$_2$O, cell-associated dye was dissolved in a 0.1% acetic acid solution in 50% ethanol. Absorbance (585 nm) was measured in a microtitre plate reader (SpectraMax-340; Molecular Devices).

Retinal explant culture. All experiments were performed in accordance with the ARVO Statement for Use of Animals in Ophthalmic and Vision Research. C57BL/6 mice were obtained from Harlan UK (Bicester, UK). Briefly, C57BL/6 mice were decapitated at P10 and the eyes were removed. The anterior segment, vitreous body and sclera were removed and the retina was mounted on nitrocellulose inserts (Millicell; Millipore, Billerica, MA, USA) with photoreceptor facing down. Explants were cultured without retinal pigment epithelium in 1.2 ml of R16 medium (from Dr. PA Ekstrom, Wallenberg Retina Centre, Lund University, Lund, Sweden) without additional serum. Treated explants were cultured in media containing 50, 150, 300 or 600 μM H$_2$O$_2$ for the indicated times. Explants were then subjected to western blotting as previously described (see western blotting).

TUNEL. Retinal explants were fixed in 10% neutral-buffered formalin overnight at 4°C, followed by cryoprotection in 25% sucrose overnight at 4°C. Frozen sections (7 μm) were incubated with terminal deoxynucleotidyl transferase (MSC, Dublin, Republic of Ireland) and fluorescein-12-dUTP (Roche, Lewes, UK) according to the manufacturer's instructions at 37°C for 1 h. Nuclei were counterstained (Hoechst 33342; Sigma). Sections were mounted and viewed under a fluorescence microscope (Leica DM LB; Leica, Nussloch, Germany) using an FITC filter.

1. Izzotti A, Bagnis A, Sacca SC. The role of oxidative stress in glaucoma. *Mutat Res* 2006; **612**: 105–114.
2. Andersen J. Oxidative stress in neurodegeneration: cause or consequence? *Nat Rev Neurosci* 2004; **5**: S18–S25.
3. Zoccarato F, Toscano P, Alexandre A. Dopamine-derived dopaminochrome promotes H(2)O(2) release at mitochondrial complex I: stimulation by rotenone, control by Ca(2+), and relevance to Parkinson disease. *J Biol Chem* 2005; **280**: 15587–15594.
4. Behl C, Davis JB, Lesley R, Schubert D. Hydrogen peroxide mediates amyloid β protein toxicity. *Cell* 1994; **77**: 817–827.
5. Spector A. Oxidative stress-induced cataract: mechanism of action. *FASEB J* 1995; **9**: 1173–1182.
6. Bailey TA, Kanuga N, Romero IA, Greenwood J, Luthert PJ, Cheetham ME. Oxidative stress affects the junctional integrity of retinal pigment epithelial cells. *Invest Ophthalmol Vis Sci* 2004; **45**: 675–684.
7. Chandra J, Samali A, Orrenius S. Triggering and modulation of apoptosis by oxidative stress. *Free Radic Biol Med* 2000; **29**: 323–333.
8. Finkel T, Holbrook N. Oxidants, oxidative stress and the biology of ageing. *Nature* 2000; **408**: 239–247.
9. Finkel T. Oxidant signals and oxidative stress. *Curr Opin Cell Biol* 2003; **15**: 247–254.
10. Hancock JT, Desikan R, Neill SJ. Role of reactive oxygen species in cell signalling pathways. *Biochem Soc Trans* 2001; **29**: 345–350.
11. Giniatullin AR, Grishin SN, Sharifullina ER, Petrov AM, Zefirov AL, Giniatullin RA. Reactive oxygen species contribute to the presynaptic action of extracellular ATP at the frog neuromuscular junction. *J Physiol* 2005; **565**: 229–242.
12. Auerbach AM, Segal M. Peroxide modulation of slow onset potentiation in rat hippocampus. *J Neurosci* 1997; **17**: 8695–8701.
13. Nemoto S, Takeda K, Yu ZX, Ferrans VJ, Finkel T. Role for mitochondrial oxidants as regulators of cellular metabolism. *Mol Cell Biol* 2000; **20**: 7311–7318.
14. Casas J, Gorchs G, Sanchez-Baeza F, Teixidor P, Messeguer A. Inhibition of rat liver microsomal lipid peroxidation elicited by simple 2,2-dimethylchromenes and chromans structurally related to precocenes. *J Agric Food Chem* 1992; **40**: 585–590.
15. England K, O'Driscoll C, Cotter TG. Carbonylation of glycolytic proteins is a key response to drug-induced oxidative stress and apoptosis. *Cell Death Differ* 2004; **11**: 252–260.
16. Gorman A, McGowan A, Cotter TG. Role of peroxide and superoxide anion during tumour cell apoptosis. *FEBS Lett* 1997; **404**: 27–33.
17. Sanvicens N, Gomez-Vicente V, Messeguer A, Cotter TG. The radical scavenger CR-6 protects SH-SY5Y neuroblastoma cells from oxidative stress-induced apoptosis: effect on survival pathways. *J Neurochem* 2006; **98**: 735–747.
18. Seo JH, Ahn Y, Lee SR, Yeol Yeo C, Chung Hur K. The major target of the endogenously generated reactive oxygen species in response to insulin stimulation is phosphatase and tensin homolog and not phosphoinositide-3 kinase (PI-3 kinase) in the PI-3 kinase/Akt pathway. *Mol Biol Cell* 2005; **16**: 348–357.
19. Lee SR, Yang KS, Kwon J, Lee C, Jeong W, Rhee SG. Reversible inactivation of the tumor suppressor PTEN by H$_2$O$_2$. *J Biol Chem* 2002; **277**: 20336–20342.
20. Stambolic V, Suzuki A, de la Pompa JL, Brothers GM, Mirtsos C, Sasaki T *et al.* Negative regulation of PKB/Akt-dependent cell survival by the tumor suppressor PTEN. *Cell* 1998; **95**: 29–39.
21. Wu X, Senechal K, Neshat MS, Whang YE, Sawyers CL. The PTEN/MMAC1 tumor suppressor phosphatase functions as a negative regulator of the phosphoinositide 3-kinase/Akt pathway. *Proc Natl Acad Sci USA* 1998; **95**: 15587–15591.
22. Bae YS, Sung JY, Kim OS, Kim YJ, Hur KC, Kazlauskas A *et al.* Platelet-derived growth factor-induced H(2)O(2) production requires the activation of phosphatidylinositol 3-kinase. *J Biol Chem* 2000; **275**: 10527–10531.
23. Colavitti R, Pani G, Bedogni B, Anzevino R, Borrello S, Waltenberger J *et al.* Reactive oxygen species as downstream mediators of angiogenic signaling by vascular endothelial growth factor receptor-2/KDR. *J Biol Chem* 2002; **277**: 3101–3108.
24. Chipuk JE, Bouchier-Hayes L, Green DR. Mitochondrial outer membrane permeabilization during apoptosis: the innocent bystander scenario. *Cell Death Differ* 2006; **13**: 1396–1402.
25. Donovan M, Carmody RJ, Cotter TG. Light-induced photoreceptor apoptosis *in vivo* requires neuronal nitric-oxide synthase and guanylate cyclase activity and is caspase-3-independent. *J Biol Chem* 2001; **276**: 23000–23008.
26. Gomez-Vicente V, Donovan M, Cotter TG. Multiple death pathways in retina-derived 661W cells following growth factor deprivation: crosstalk between caspases and calpains. *Cell Death Differ* 2005; **12**: 796–804.
27. Doonan F, Donovan M, Cotter TG. Activation of multiple pathways during photoreceptor apoptosis in the rd mouse. *Invest Ophthalmol Vis Sci* 2005; **46**: 3530–3538.
28. Sanvicens N, Cotter TG. Ceramide is the key mediator of oxidative stress-induced apoptosis in retinal photoreceptor cells. *J Neurochem* 2006; **98**: 1432–1444.
29. Harada T, Harada C, Nakamura K, Quah HM, Okumura A, Namekata K *et al.* The potential role of glutamate transporters in the pathogenesis of normal tension glaucoma. *J Clin Invest* 2007; **117**: 1763–1770.
30. Doonan F, Donovan M, Gomez-Vicente V, Bouillet P, Cotter TG. Bim expression indicates the pathway to retinal cell death in development and degeneration. *J Neurosci* 2007; **27**: 10887–10894.
31. Tanito M, Kwon YW, Kondo N, Bai J, Masutani H, Nakamura H *et al.* Cytoprotective effects of geranylgeranylacetone against retinal photooxidative damage. *J Neurosci* 2005; **25**: 2396–2404.
32. Schlieve CR, Lieven CJ, Levin LA. Biochemical activity of reactive oxygen species scavengers do not predict retinal ganglion cell survival. *Invest Ophthalmol Vis Sci* 2006; **47**: 3878–3886.
33. Mahadev K, Wu X, Zilbering A, Zhu L, Lawrence JTR, Goldstein BJ. Hydrogen peroxide generated during cellular insulin stimulation is integral to activation of the distal insulin signaling cascade in 3T3-L1 adipocytes. *J Biol Chem* 2001; **276**: 48662–48669.
34. Tonks NK. Redox redux: revisiting PTPs and the control of cell signaling. *Cell* 2005; **121**: 667–670.
35. Datta SR, Dudek H, Tao X, Masters S, Fu H, Gotoh Y *et al.* Akt phosphorylation of BAD couples survival signals to the cell-intrinsic death machinery. *Cell* 1997; **91**: 231–241.
36. Cardone MH, Roy N, Stennicke HR, Salvesen GS, Franke TF, Stanbridge E *et al.* Regulation of cell death protease caspase-9 by phosphorylation. *Science* 1998; **282**: 1318–1321.
37. Moncada S, Erusalimsky JD. Does nitric oxide modulate mitochondrial energy generation and apoptosis? *Nat Rev Mol Cell Biol* 2002; **3**: 214–220.
38. Wang X, McCullough K, Franke T, Holbrook N. Epidermal growth factor receptor-dependent Akt activation by oxidative stress enhances cell survival. *J Biol Chem* 2000; **275**: 14624–14631.
39. Tang XQ, Feng JQ, Chen J, Chen PX, Zhi JL, Cui Y *et al.* Protection of oxidative preconditioning against apoptosis induced by H$_2$O$_2$ in PC12 cells: mechanisms via MMP, ROS, and Bcl-2. *Brain Res* 2005; **1057**: 57–64.
40. Chen ZH, Yoshida Y, Saito Y, Niki E. Adaptation to hydrogen peroxide enhances PC12 cell tolerance against oxidative damage. *Neurosci Lett* 2005; **383**: 256–259.